

REFRACTION—DIFFRACTION OF IRREGULAR WAVES OVER A MOUND

By Charles L. Vincent,¹ Member, ASCE, and Michael J. Briggs,² Member, ASCE

ABSTRACT: The transformation of monochromatic and directionally-spread irregular waves passing over a submerged elliptical mound was studied in a controlled laboratory experiment. A directional spectral wave generator was used to generate waves with equal peak frequencies and spectral energy, along with monochromatic waves of equivalent significant height and period. Spectra with both narrow and broad frequency and directional spreads were generated. Results indicate that monochromatic waves provide a poor approximation of irregular wave conditions if there is directional spread or high wave steepness.

INTRODUCTION

Estimation of the refraction and diffraction of waves passing over complicated bathymetry has been a persistent problem in coastal engineering. Although the complexity of natural wave systems is recognized, most engineering analyses of wave propagation over irregular bathymetry have been based on representation of seastate by a monochromatic wave of height, period, and direction usually chosen to approximate the significant wave. The propagation problem is solved either empirically in a scaled physical model or numerically by linear and, more recently, nonlinear approximations. The use of advanced propagation models rose out of the need to avoid caustics that arise in linear calculations. These numerical methods have been successful at replicating monochromatic wave propagation over severe bottom curvatures in laboratory tests (Berkhoff et al. 1982, Ebersole 1985). Spectral models for wave propagation exist in varying degrees of complexity, but are generally based on linear wave theory for propagation of individual wave components and are rarely employed on grid meshes with the resolution of the monochromatic techniques. The monochromatic approximation for spectral wave conditions inherently assumes that the representation is adequate, or at least conservative.

The development of a wavemaker at the U.S. Army Engineer Waterways Experiment Station's Coastal Engineering Research Center (CERC) capable of generating a controlled directional spectrum allows investigation of the adequacy of the monochromatic approximation for simulating propagation of natural seastates over irregular bathymetry. The bathymetry for the tests was an elliptical shoal similar to that of Berkhoff et al. (1982). The concept of the experimental design was to select a monochromatic wave of height H , period T , and direction θ that would represent a seastate of significant height H_s , peak period T_p , and overall mean wave direction $\bar{\theta}$. It is possible

¹Sr. Sci., Coastal Engrg. Res. Cr., USAE Waterways Experiment Station, P.O. Box 631, Vicksburg, MS 39180-0631.

²Res. Hydr. Engr., Coastal Engrg. Research Center, USAE Waterways Experiment Sta., Vicksburg, MS.

Note. Discussion open until August 1, 1989. To extend the closing date one month, a written request must be filed with the ASCE Manager of Journals. The manuscript for this paper was submitted for review and possible publication on July 20, 1988. This paper is part of the *Journal of Waterway, Port, Coastal, and Ocean Engineering*, Vol. 115, No. 2, March, 1989. ©ASCE, ISSN 0733-950X/89/0002-0269/\$1.00 + \$.15 per page. Paper No. 23311.

to create an infinite number of directional spectra $S(f, \theta)$ with the H_s , T_p , and $\bar{\theta}$ required, and an infinite number of time history realizations for each spectrum. The scope of this research was confined to four combinations of narrow and broad frequency and directional spreading representative of naturally occurring wave environments. A total of 17 test cases were run. The variation of height, period, and direction in the basin was represented as $H(x, y)$, $T(x, y)$, and $\theta(x, y)$, respectively. Corresponding normalized quantities $A = H(x, y)/H_o$, $B = T(x, y)/T_o$, and $C = \theta(x, y)/\theta_o$ were formed by dividing by the incident condition (assumed to be uniform along the wavemaker). For the irregular waves, H_s , T_p , and $\bar{\theta}$ are used in A , B , and C . Monochromatic tests are denoted by a subscript m (A_m, B_m, C_m) and irregular tests by subscript i (A_i, B_i, C_i). The experiment consisted of generating and measuring waves and then forming the quantities A , B , and C for a large number of locations in the basin. Any difference between A_m , B_m , C_m , and A_i , B_i , C_i provides a measure of the divergence of the monochromatic approximation to natural seastates. Differences among A_i , B_i , and C_i for the spectral cases would indicate the relative importance of directional versus frequency spread. This paper reports on wave height only. The period patterns showed little variation. The directional analysis is more difficult and requires separate treatment.

Although the conceptual design is simple, underlying assumptions and implicit decisions are made that should be recognized at the outset. First, Thompson and Vincent (1985) reported the difficulty of comparing irregular and monochromatic waves, pointing out that one can match varying combinations of H_{mo} and H_s for the irregular waves with H_{mo} and H for the monochromatic. Here, H_{mo} and H were matched, which would be the typical engineering approach. In any case, the differences between A_i based on H_{mo} and A_i based on H_s were small. Second, with irregular waves, random superposition can cause wave breaking that would not occur with small monochromatic waves. This is an essential feature of irregular waves in nature, so cases were selected in which breaking was not a dominant feature and an attempt to quantify its effect was made. Third, although the irregular wave conditions were reasonably consistent along the wavemaker, the finite length of the wavemaker restricts the region in the basin over which homogeneity can be assumed, even when a shoal is not present. Finally, only one realization per spectrum was generated, but that realization was generally repeated several times to quantify experimental consistency. This is quite different from selecting additional realizations.

This experiment allowed quantification of the differences between the refraction/diffraction patterns of a monochromatic wave and irregular seastates of similar summary statistics, and some definition of the parameters causing these differences. The tests by no means exhaust the possibilities of the general problem of refraction and diffraction of irregular waves, but serve as a first attempt to identify important factors for further experiments. Coincidentally, data for verifying irregular wave propagation models were obtained.

TEST SET-UP

The shoal tests were conducted in CERC's 35 m (114 ft) wide by 29 m (96 ft) long directional spectral wave basin. The bathymetry (Briggs and

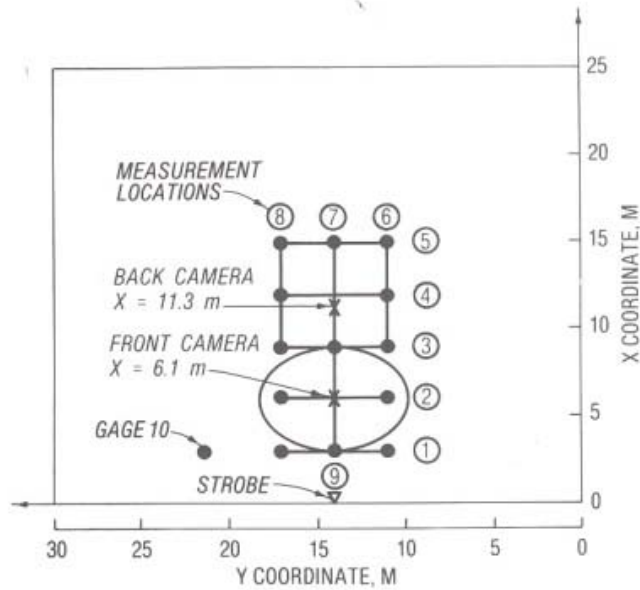


FIG. 1. Locations of Elliptical Shoal and Measurement Transects

Hampton 1987) is uniform with a maximum variation of 9 mm (0.35 in.). The perimeter is lined with wave absorber frames that provide sufficient wave energy attenuation to prevent adverse reflections.

Waves are generated with the directional spectral wave generator (DSWG). It is 27.43 m (90 ft) long and consists of 60 paddles in four portable modules, each 46 cm (1.5 ft) wide and 76 cm (2.5 ft) high. The paddles are individually driven at each of the 61 joints in translational motion by electric motors using the "snake principle." Flexible plastic plate seals slide in guides between each paddle to provide continuity (Outlaw 1984).

A 6.10 m (20 ft) wide by 15.24 m (50 ft) long measurement area was centrally located in front of the DSWG (Fig. 1). The center of the shoal was located at coordinates $x = 6.10$ m (20 ft) and $y = 13.72$ m (45 ft). Surface elevation time histories were measured using an array of nine parallel-wire resistance-type sensors. They were spaced 76 cm (2.5 ft) apart in an aluminum frame that minimized the amount of interference from support legs. Fig. 1 illustrates the nine positions (5 parallel to the DSWG and 4 perpendicular) within the measurement area. A tenth gage was located at $X = 3.05$ (10 ft) and $Y = 21.34$ m (70 ft) as a reference gage for normalizing. Photographic and cinematographic records of the patterns created by the different wave conditions were recorded from an overhead catwalk located parallel to the DSWG at $X = 9.14$ m (30 ft).

The elliptical shoal was patterned after Berkhoff et al. (1982) with a major radius of 3.96 m (13 ft), minor radius of 3.05 m (10 ft), and a maximum height of 30.48 cm (1 ft) at the center. It was constructed with sand between aluminum ribs and had a 5.08 cm (2 inch) mortar cap (Fig. 2). The shoal boundary or perimeter is defined by

$$\left(\frac{X'}{3.05}\right)^2 + \left(\frac{Y'}{3.96}\right)^2 = 1 \dots\dots\dots (1)$$

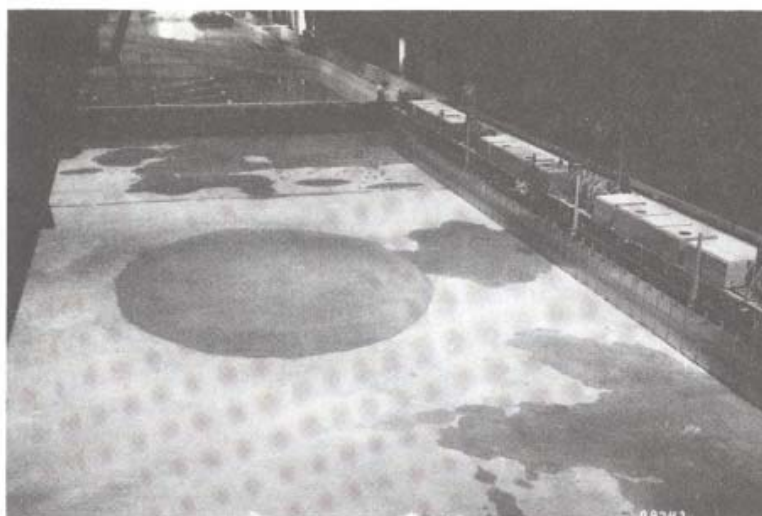


FIG. 2. Photograph of Elliptical Shoal and Directional Spectral Wave Generator

where X' and Y' are localized coordinates centered on the shoal denoting minor and major axes, respectively. The elevation at any point in the shoal cross-section E_s , in meters is given by

$$E_s = -0.4572 + 0.7620 \left\{ 1 - \left(\frac{X'}{3.81} \right)^2 - \left(\frac{Y'}{4.95} \right)^2 \right\}^{0.5} \dots\dots\dots (2)$$

All tests were run in 45.72 cm (1.5 ft) water depth h so the distance at the center of the shoal to still water level was 15.24 cm (0.5 ft).

CONTROL SIGNAL GENERATION

A Digital Vax 11/750 was used to generate and transmit the control signals, monitor DSWG feedback, and collect, analyze, and store wave data. For the monochromatic waveforms, the governing equation for the control signal S_c to each of the 61 DSWG paddles at location y and time t is

$$S_c(y, t) = \frac{S}{2} \cos (2\pi ft + \phi_y) \dots\dots\dots (3)$$

in which S = double amplitude stroke; f = frequency; and ϕ_y = offset phase controlling wave direction, 0 for waves in this study. This time series is multiplied by the height-to-stroke transfer function H/S for this frequency to obtain the desired wave height in the basin (Biesel 1954, Sand 1979).

The directional wave spectrum $S(f, \theta)$ was defined as

$$S(f, \theta) = S(f)D(f, \theta) \dots\dots\dots (4)$$

in which $S(f)$ = a one-dimensional frequency spectrum given by

$$S(f) = \int_0^{2\pi} S(f, \theta) d\theta \dots\dots\dots (5)$$

and $D(f, \theta) =$ a directional spreading function that satisfies

$$\int_0^{2\pi} D(f, \theta) d\theta = 1 \dots\dots\dots (6)$$

The TMA shallow-water spectral form (Bouws et al. 1985) was selected as the target frequency spectrum, and a wrapped normal function was used for the directional spreading function (Borgman 1984). The TMA spectrum (named for the Texel, MARSEN and ARSLOE data sets) is a function of five parameters: peak frequency f_p , alpha constant α , peak enhancement factor γ , spectral width parameter σ , and water depth h . A Fourier series representation for the wrapped normal spreading function is

$$D(f, \theta) = \frac{1}{2\pi} + \frac{1}{\pi} \sum_{l=1}^L \exp \left\{ -\frac{(l\sigma_m)^2}{2} \right\} \cos l(\theta - \theta_m) \dots\dots\dots (7)$$

in which $\theta_m =$ mean wave direction at frequency f ; $\sigma_m =$ directional spreading parameter or spreading standard deviation at frequency f ; and $L =$ arbitrary number of harmonics chosen to represent the Fourier series.

Realizations of a desired time series for directional wave spectrum for each of the 61 DSWG paddles were simulated in the frequency domain using a deterministic amplitude, random phase method (Briggs et al. 1987). A uniform Gaussian white noise spectrum is multiplied by the target TMA spectrum to give a sample spectrum. The method is equivalent to filtering the Gaussian signal in the frequency domain. The pseudointegral model for the irregular, random surface elevation time series η is

$$\eta(x, y, t) = 2 \sum_{m=1}^M \sum_{j=1}^J A_{mj} \cos (k_m x \cos \theta_j + k_m y \sin \theta_j - 2\pi f_m t + \phi_{mj}) \dots\dots (8)$$

in which x and $y =$ coordinates of each of the 61 DSWG paddles; $t =$ incremental time step $= n\Delta t$; $A_{mj} =$ deterministic amplitude of a wave traveling in θ_j direction $= \sqrt{2S(f, \theta)df d\theta}$; and $\phi_{mj} =$ random phase, independent over frequency and direction and uniformly distributed over the interval $(0, 2\pi)$. The simulated directional spectrum is adjusted, if needed, to match a specified input variance for the spectrum. The amplitudes in Eq. 8 can be related to the Fourier coefficients and inverted rapidly, using a "235" fast Fourier transform (FFT) to obtain the desired time series. The length of the time series N must be a product of the powers of 2, 3, and 5 such that

$$N = 2^K 3^L 5^M \dots\dots\dots (9)$$

These random wave realizations are then multiplied by a constant dimensionless wavemaker frequency response function to obtain the desired DSWG stroke time series.

For wave generation, an A/D rate of 20 Hz was used. The lower and upper frequency cutoffs used were 0.5 and 1.50 Hz, respectively. The overall mean wave direction $\bar{\theta}$ for all test cases was 0°

TEST CONDITIONS

The total test program reported in this paper consisted of 17 test cases. An initial series of test conditions comprised five cases: one monochromatic

TABLE 1. Test Conditions for Shoal Test Series

Test number (1)	Case ID (2)	Type (3)	Period (sec) (4)	Height (cm) (5)	α (6)	γ (7)	σ_m (deg) (8)
(a) Initial Series							
1	M1	Mono	1.30	5.50	—	—	—
2	N1	Spec	1.30	7.75	0.01440	2	10
3	B1	Spec	1.30	7.75	0.01440	2	30
4	N2	Spec	1.30	7.75	0.00440	20	10
5	B2	Spec	1.30	7.75	0.00440	20	30
(b) Unidirectional Series							
6	U1	Spec	1.30	7.75	0.01440	2	0
7	U2	Spec	1.30	7.75	0.00440	20	0
(c) Non-Breaking Series							
8	M2	Mono	1.30	2.54	—	—	—
9	U3	Spec	1.30	2.54	0.00155	2	0
10	N3	Spec	1.30	2.54	0.00155	2	10
11	B3	Spec	1.30	2.54	0.00155	2	30
12	U4	Spec	1.30	2.54	0.00047	20	0
13	N4	Spec	1.30	2.54	0.00047	20	10
14	B4	Spec	1.30	2.54	0.00047	20	30
(d) Breaking Series							
15	M3	Mono	1.30	13.50	—	—	—
16	B5	Spec	1.30	19.00	0.08650	2	30
17	N5	Spec	1.30	19.00	0.02620	20	10

(M1) and four (N1, B1, N2, and B2) directional spectral ($N =$ narrow and $B =$ broad directional spreading). Equivalent wave heights were used in this series. Based on the results from this initial series, 12 additional cases were generated to investigate the effects of different factors, including directional spreading, wave amplitude, and breaking. These additional cases were measured on Transect 4 only. Table 1 summarizes the wave parameters for each of these cases.

For the M1 monochromatic case, an equivalent wave height relative to the spectral height was defined by

$$\frac{H_{m0}}{\sqrt{2}} \dots \dots \dots (10)$$

Two TMA frequency spectra with the same peak frequency were generated. Spectral peakedness values of $\gamma = 2$ and 20 provided a broad and narrow frequency spectra, respectively. The α value was selected to give the target H_{m0} wave height. These frequency spectra were paired with narrow ($\sigma_m = 10^\circ$) and broad ($\sigma_m = 30^\circ$) directional spreading defined by Eq. 7. Figs. (3a–b) illustrate measured and predicted frequency spectra and directional spreading functions, respectively.

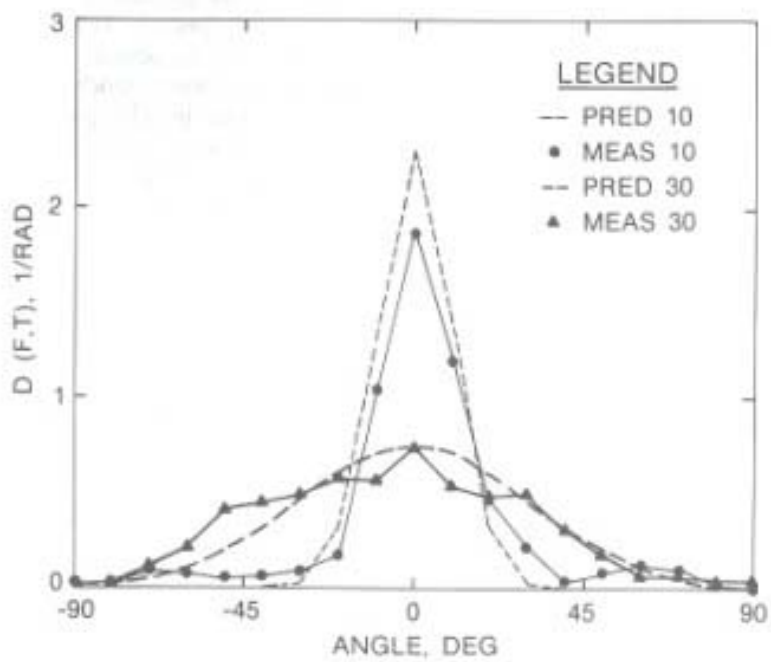
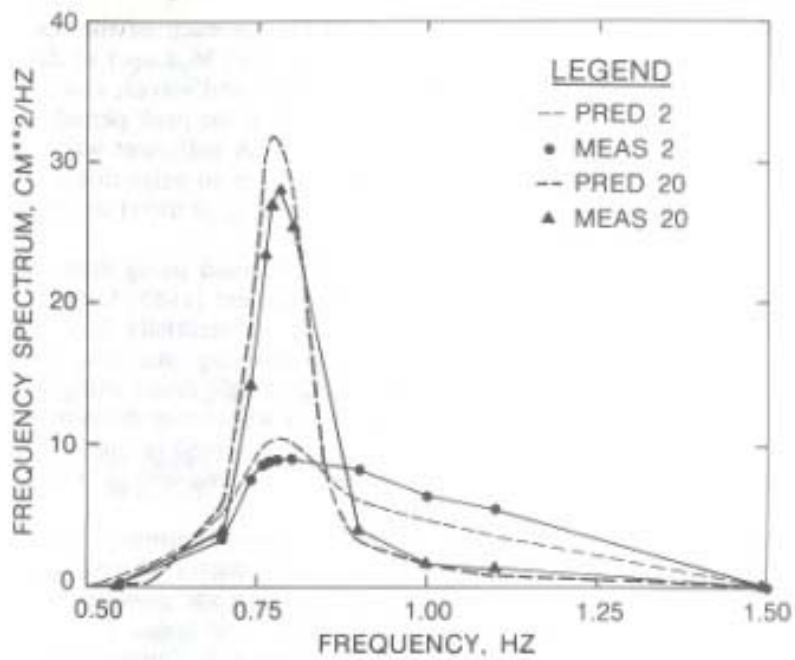


FIG. 3. (a)-(b) Measured versus Predicted Wave Spectra and Directional Spreading Functions

WAVE DATA COLLECTION AND ANALYSIS

Wave elevation data were sampled at 50 Hz for each of the ten wave gages. For the monochromatic waves, 1,820 points (36.4 sec) of data representative of 28 cycles were collected. For the spectral waves, Goda (1985) recommends collecting a minimum of 200 waves at the peak period, so 260 sec of data or 13,000 data points were measured. A sufficient waiting time was allowed to elapse after start of the DSWG prior to collection to permit the slower-traveling high frequency component waves to travel to the remote transect 5 (Fig. 1).

Wave height and period information were obtained using zero-crossing and spectral analysis methods. Thompson and Vincent (1985) found that the H_{mo} value calculated for shallow water can be substantially less than the significant wave height H_s obtained from zero-crossing analyses. With this fact in mind, a comparison of the wave heights calculated using the two different methods indicated very good agreement with minor differences only at the top of the shoal. The wave height values presented in this paper used the zero-crossing method. The H_{mo} values are documented in a report by Briggs (1987).

Frequency spectra and directional spreading were determined using a directional spectral analysis method. Prior to construction of the shoal, a spatial array of nine gages was used to obtain frequency and directional spreading characteristics of each of the spectral wave conditions. The measured surface data for each gage was zero-meaned, windowed, Fourier-transformed with the "235" FFT, and Gaussian-smoothed in the frequency domain to obtain the cross-spectral matrix of auto- and cross-spectra. This matrix is substituted into the parameterized spreading function to obtain a set of simultaneous, linear equations. A linear, stepwise regression model was used to solve for the Fourier coefficients of the spreading function (Borgman 1984).

Several runs of each test case for a particular transect were made. Cross-plots of measured heights showed a high degree of repeatability among tests for the different gage locations. Replications were typically within 5 percent of the average.

LABORATORY TEST RESULTS

Initial Series

The normalized wave height ratio A is contoured as a function of (x,y) position in the laboratory basin in Figs. 4(a-e) for the initial series of test cases 1-5. The dashed line on these figures represents the outline of the elliptical shoal. These tests ($M1$, $N1$, $N2$, $B1$, and $B2$) correspond to a monochromatic wave, and the four combinations of narrow or broad frequency and directional spreading. Although the five cases all have distinctly different patterns of wave height amplification and reduction, the difference between the monochromatic wave and irregular wave cases is dramatic. The pattern associated with monochromatic waves shows a strong convergence region behind the mound where wave height amplification reaches 2.6. There are two regions to the side in which the wave height ratio is significantly less than 0.6. The directional spectral waves, in contrast, have no amplification greater than 1.4, which is almost 50% less than the monochromatic case. Given the great difference in amplification, the narrow directional spread

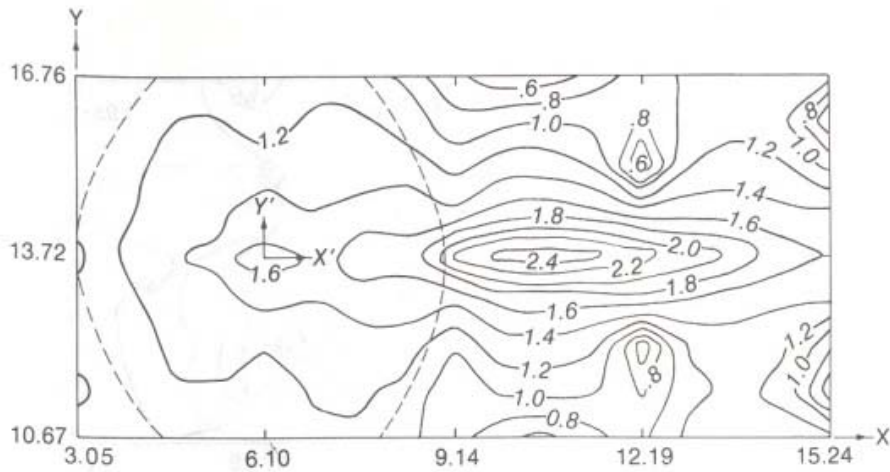


FIG. 4. (a)–(e) Three-Dimensional Surface of Normalized Wave Heights for Initial Series Test Cases 1–5

cases ($N1, N2$) have patterns most similar to the monochromatic case. The greatest contrast is between the monochromatic case, with its strong focusing, and the broad directional cases, in which the waves appear only barely perturbed in passing over the mound.

Intercomparison of the four directional spectral cases indicates that the patterns for the two narrow spread cases ($N1, N2$) are reasonably similar, and that the two broad spread cases ($B1, B2$) are likewise similar. The greatest difference in separating the spectral cases is the amount of directional spread, rather than the peakedness (spread in frequency space) of the spectrum. This difference can be seen in the plot of the normalized wave heights along transect 4, which cross close to the region of maximum amplification.

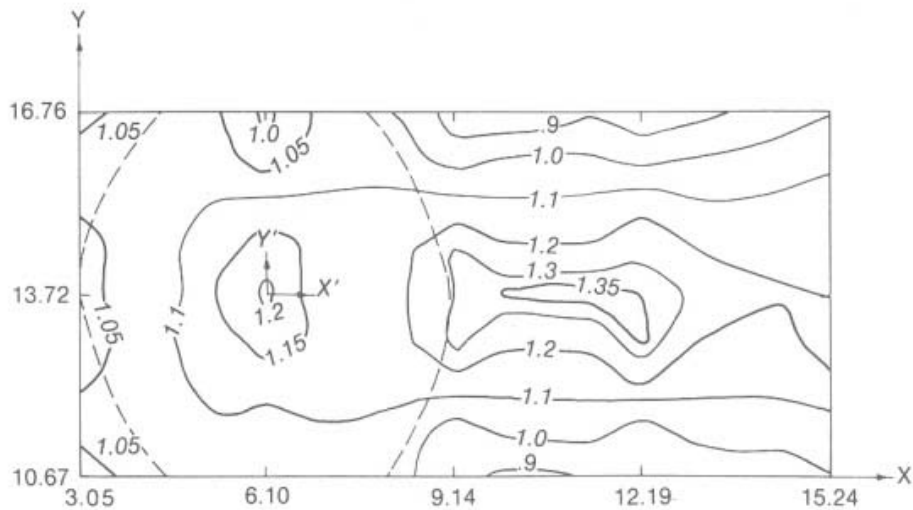


FIG. 4. (Continued)

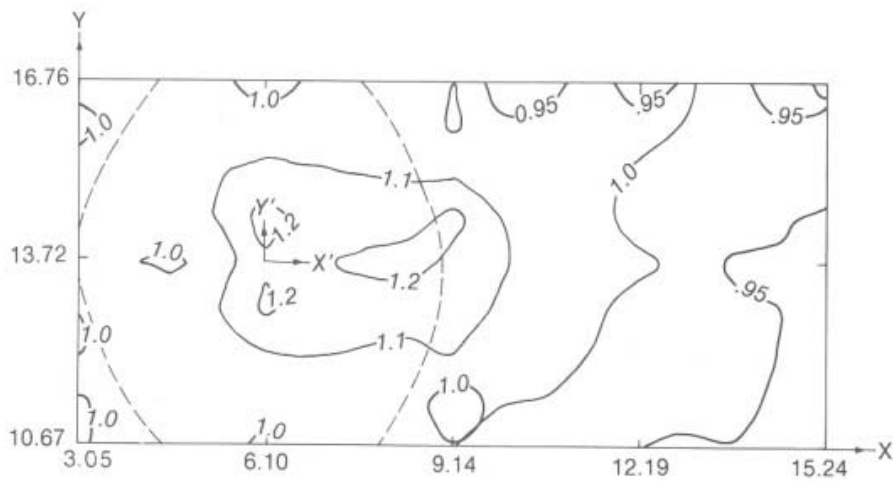


FIG. 4. (Continued)

Unidirectional Series

To further investigate the effect of directional spread, two unidirectional cases (cases 6 and 7: $U1$ and $U2$) with the same frequency spectra but no directional spreading were generated and compared to the previous five cases. Fig. 5 shows these two cases have similar patterns and are more like the monochromatic waves than the directional spread cases, although substantial differences remain.

Nonbreaking Series

At this point it was clear that the presence of directionality was of greatest significance in determining the major differences seen. In the monochromatic case, no wave breaking was observed. In the irregular wave cases, particularly with the narrow spread cases, occasional superposition of waves

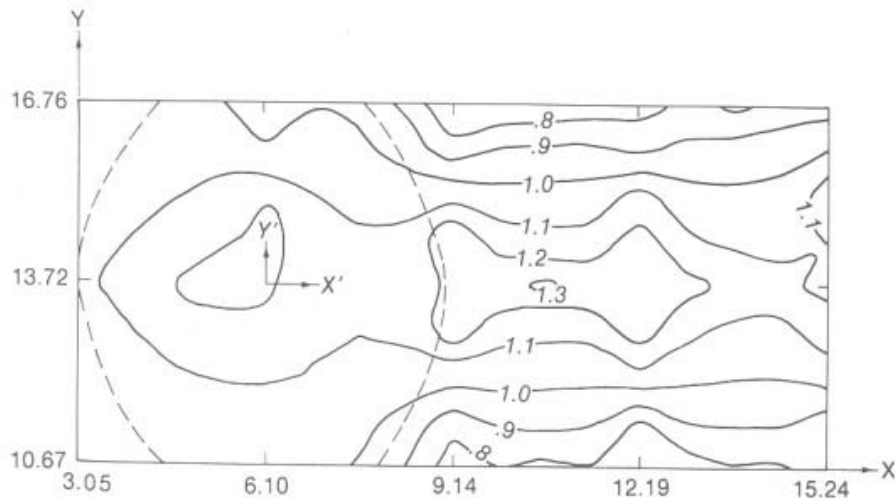


FIG. 4. (Continued)

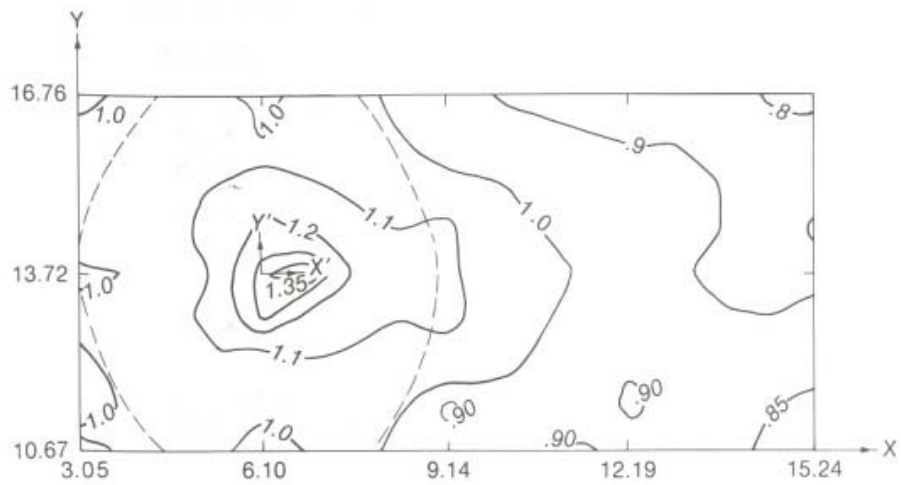


FIG. 4. (Continued)

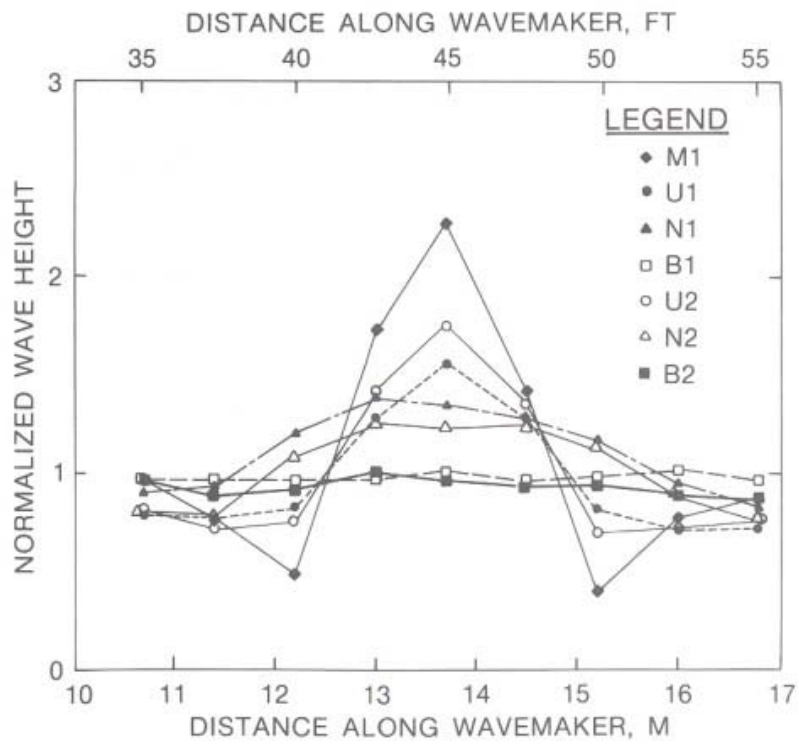


FIG. 5. Normalized Wave Heights Along Transect 4 for Initial and Unidirectional Series Test Cases 1-7

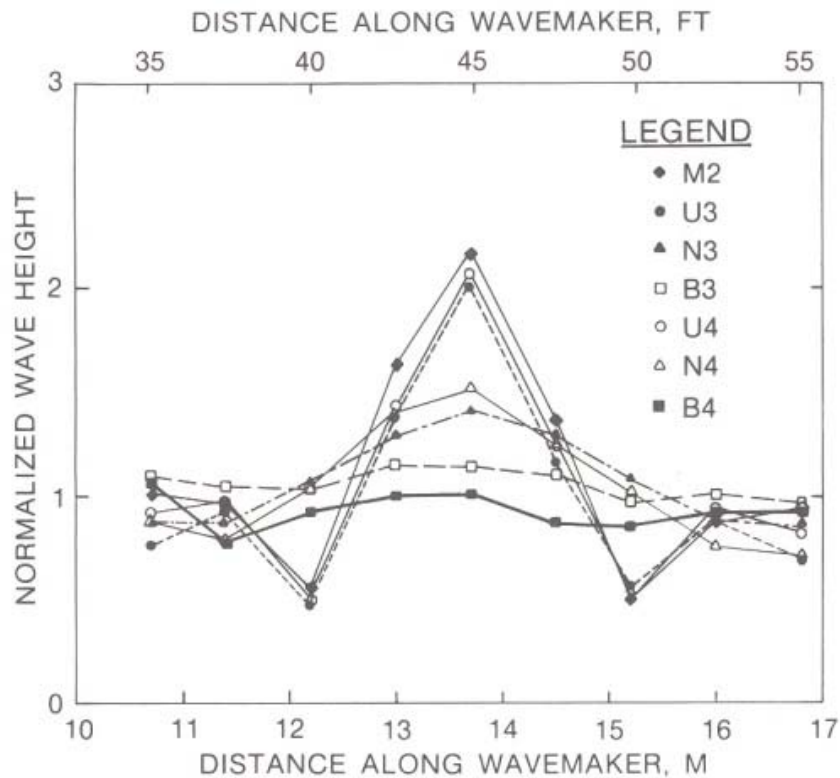


FIG. 6. Normalized Wave Heights Along Transect 4 for Non-Breaking Series Test Cases 8–14

induced some breaking in the vicinity of the mound. Although visual observation did not suggest that this was a pervasive influence on the results, seven additional tests (cases 8–14: *M2*, *U3*, *N3*, *B3*, *U4*, *N4*, and *B4*, respectively) were run with small waves in which no breaking occurred.

As in the initial series, the pattern of normalized wave height variation again grouped according to amount of directional spread (Fig. 6). Those cases with $\sigma_m = 10$ and 30° are still very different from the monochromatic case. The unidirectional case is most similar to the monochromatic case. These tests verify that directional spread in the initial cases was responsible for the dramatic differences between the four irregular wave cases and the monochromatic case.

Breaking Series

To demonstrate the effect of large scale breaking, a series of three tests (cases 15–17), one monochromatic (*M3*) and two spectral (*B5* and *N5*), were generated and measured. All had large enough wave heights to ensure significant breaking over the shoal. The two spectral cases bracketed the frequency and directional spread conditions previously tested: case *B5* with wide spreads and case *N5* with narrow (Table 1). The normalized height patterns (Fig. 7) clearly show that the shoal produces significant decrease in wave height with only minor differences in the wave height patterns. The results

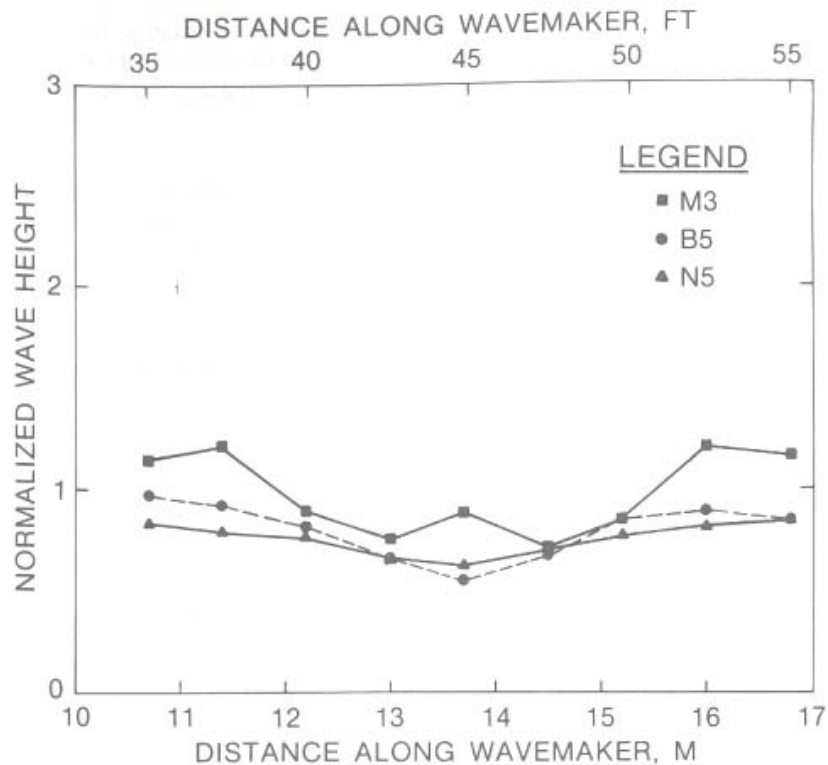


FIG. 7. Normalized Wave Heights Along Transect 4 for Breaking Series Test Cases 15-17

suggest that computing a transfer function such as A_i for nonbreaking wave conditions and then using it if breaking occurs over a shoal will be misleading.

ANALYSIS

Our objective was to establish how well a monochromatic wave represented irregular waves for the case of strong bathymetric induced wave convergence. The conclusions reached for the elliptical shoal are the following:

1. Monochromatic waves overestimate the maximum amplification of irregular waves with typical directional spreads (i.e., $\sigma_m = 10$ and 30°) by 50 to over 100%.
2. Monochromatic waves indicate existence of two divergence zones that either are not, or only minimally, present for irregular waves with typical directional spreads. As a consequence, the monochromatic waves underestimate wave heights by up to 50% in these zones.
3. The degree of directional spread in the irregular wave cases is a more significant parameter than the spread of energy in frequency space, for the cases modeled.
4. Both the monochromatic and irregular wave height amplification patterns are sensitive to incident wave height.

5. The monochromatic wave tests provide a good representation (error of 5–10%) of the irregular cases only if the waves are unidirectional and small. The situation of no directional spread may be artificial and unlikely to occur outside the laboratory.

The elliptical shoal is one of the classic examples by which the inadequacy of linear monochromatic wave ray theory has been illustrated in the past, and is one basis on which more sophisticated monochromatic wave propagation models have been judged. Our results indicate that monochromatic waves are a poor substitute for irregular waves if realistic directional spreads are present for the case of irregular bathymetry.

The tests examined one mound and a range of spectral conditions that represent, to some degree, the extremes of spectral shape for a single peak spectrum. It is not possible to address definitively the general problem of irregular wave propagation over an arbitrary bottom. However, some points are relevant to the use of monochromatic waves to represent natural sea-states. First, if the bathymetry produces strong wave convergence, it seems unlikely that a monochromatic approach will provide accurate results. Second, refraction-diffraction patterns are sensitive to wave amplitude, and hence it may be unwise to compute a refraction–diffraction solution for a unit wave height and use a transfer function approach if large waves are to be calculated. Third, the differences are minimized only if the condition of no spread and low amplitude is satisfied.

Test results indicate that directional spreading has a substantial effect. High quality directional information appears to be a prerequisite for accurate engineering design. Such data are not generally available from measurements, and wave hindcast directional resolutions are usually too broad. Consequently, selection of an appropriate directional spread may require considerable judgment for which little data or experience is available.

These tests were an initial examination of the problem of refraction–diffraction of irregular wave trains. From the experimental point of view, the results were reproducible in repetitive tests, and the significant differences observed exceeded error levels due to measurement reproducibility. With spectral conditions in particular, it is difficult to assure exactness of replication, and some small differences may be due to randomness of the phenomena. The tests do not represent an exhaustive examination of all possible directional spreads and frequency spectrum shapes. However, they do span a fairly wide range in shapes, spreads, and energy levels for a fixed peak period. Thus, the implications of the difference found are likely to apply to a range of natural conditions.

SUMMARY

Experiments were conducted with the CERC directional spectral wave generator to examine the difference in the pattern of wave heights behind an elliptical shoal for monochromatic and irregular waves of similar height, period, and mean direction. The test results indicate that monochromatic waves deviate by as much as 50 to over 100% from irregular waves with typical spectral shapes and directional spreads. Investigation of the cause of the difference included relative amounts of frequency and directional spread-

ing in the spectrum, steepness effects, and breaking. The most significant factor was the amount of directional spread.

ACKNOWLEDGMENTS

The authors wish to acknowledge the Office, Chief of Engineers, U.S. Army Corps of Engineers, for authorizing publication of this paper. It was prepared as part of the Laboratory Simulation of Spectral and Directional Spectral Waves work unit, in the Coastal Flooding and Storm Protection Program of the Civil Works Research and Development Program. We would like to thank Ms. Mary L. Hampton and Mr. Larry Davis for their assistance in the data reduction, and Mr. Larry Barnes for coordinating the construction of the elliptical shoal. Contributions by Dr. Leon Borgman, University of Wyoming, to the project and fruitful discussions are also recognized.

APPENDIX I. REFERENCES

- Berkhoff, J. C. W., Booy, N., and Radder, A. C. (1982). "Verification of numerical wave propagation models for simple harmonic linear water waves." *Coastal Eng.*, 6(3), 255-279.
- Biesel, F. (1954). "Wave machines." *Proc. of the First Conference on Ships and Waves*, Council on Wave Research and Society of Naval Architects and Marine Engineers, Hoboken, NJ, 288-304.
- Borgman, L. E. (1984). "Directional spectrum estimation for the S_{α} gauges." *Technical Report*, Coastal Engng. Res. Cr., USAE Waterways Experiment Station, Vicksburg, MS, 1-104.
- Bouws, E., Gunther, H., Rosenthal, W., and Vincent, C. (1985). "Similarity of the wind wave spectrum in finite depth water." *J. Geophys. Res.*, 90(C1), 975-986.
- Briggs, M. J. (1987). "Summary of WET shoal test results." Unpublished Memorandum for Record, October 26, Coastal Engng. Res. Cr., USAE Waterways Experiment Station, Vicksburg, MS.
- Briggs, M. J., and Hampton, M. L. (1987). "Directional spectral wave generator basin response to monochromatic waves." *Technical Report CERC 87-6*, Coastal Engng. Res. Cr., USAE Waterways Experiment Station, Vicksburg, MS, 1-90.
- Briggs, M. J., Borgman, L. E., and Outlaw, D. G. (1987). "Generation and analysis of directional spectral waves in a laboratory basin." *Offshore Technology Conference*, Paper OTC 5416, Houston, TX, 495-502.
- Ebersole, B. A. (1985). "Refraction-Diffraction model for linear water waves." *J. Wtrway., Port, Coast. and Oc. Engrg.*, ASCE, 3(6), 939-953.
- Goda, Y. (1985). *Random seas and design of maritime structures*. University of Tokyo Press, Japan, 1-323.
- Outlaw, D. G. (1984). "A portable directional irregular wave generator for wave basins." *Symp. on description and modeling of directional seas*, Paper No. B-3, Technical University of Denmark, B3-1-B3-8.
- Sand, S. E. (1979). "Three-Dimensional Deterministic Structure of Ocean Waves." Series Paper No. 24, Inst. of Hydrodynamics and Hydr. Engrg., Technical University of Denmark, 1-177.
- Thompson, E. F., and Vincent, C. L. (1985). "Significant wave height for shallow water design." *J. Wtrway., Port, Coast. and Oc. Engrg.*, ASCE, 111(5), 828-842.

APPENDIX II. NOTATION

The following symbols are used in this paper:

A = normalized wave height;

A_{mj}	=	deterministic spectral amplitude;
B	=	normalized wave period;
C	=	normalized wave direction;
$D(f, \theta)$	=	directional spreading function;
E_s	=	elevation along shoal cross-section;
f	=	frequency;
f_p	=	spectral peak frequency;
H	=	wave height;
H_o	=	incident wave height;
H_{m0}	=	zero-moment wave height;
H_s	=	significant wave height;
H/S	=	height-to-stroke ratio;
h	=	water depth;
k	=	wave number;
L	=	number of harmonics in Fourier series;
N	=	length of time series;
n	=	time domain summation index;
S	=	double amplitude stroke;
$S_c(y, t)$	=	wavemaker stroke control signal;
$S(f)$	=	frequency spectrum;
$S(f, \theta)$	=	directional wave spectrum;
T	=	wave period;
T_o	=	incident wave period;
T_p	=	spectral peak period;
t	=	time;
X	=	global coordinate direction;
X'	=	shoal minor axis;
x	=	x -axis coordinate;
Y	=	global coordinate direction;
Y'	=	shoal major axis;
y	=	y -axis coordinate;
α	=	TMA spectral parameter;
γ	=	peak enhancement factor;
Δt	=	time step;
η	=	irregular, random surface elevation;
θ	=	wave direction;
$\bar{\theta}$	=	overall mean wave direction;
θ_m	=	mean wave direction at frequency f ;
θ_0	=	incident wave direction;
σ	=	TMA spectral width;
σ_m	=	directional spreading standard deviation at frequency f ;
ϕ_{mj}	=	random phase; and
ϕ_y	=	offset phase angle for wavemaker.

Subscripts

c	=	control signal;
i	=	irregular wave;
j	=	summation index for direction;
m	=	summation index for frequency; monochromatic wave; mean;
p	=	peak;
s	=	spectral; shoal; and
O	=	incident condition.

Errata Journal Paper

We discovered a couple of minor mistakes in Figures 6 and 7 in the paper and report (see attached pages). The hand-written notes on the report pages are the equivalent symbols used in the journal paper.

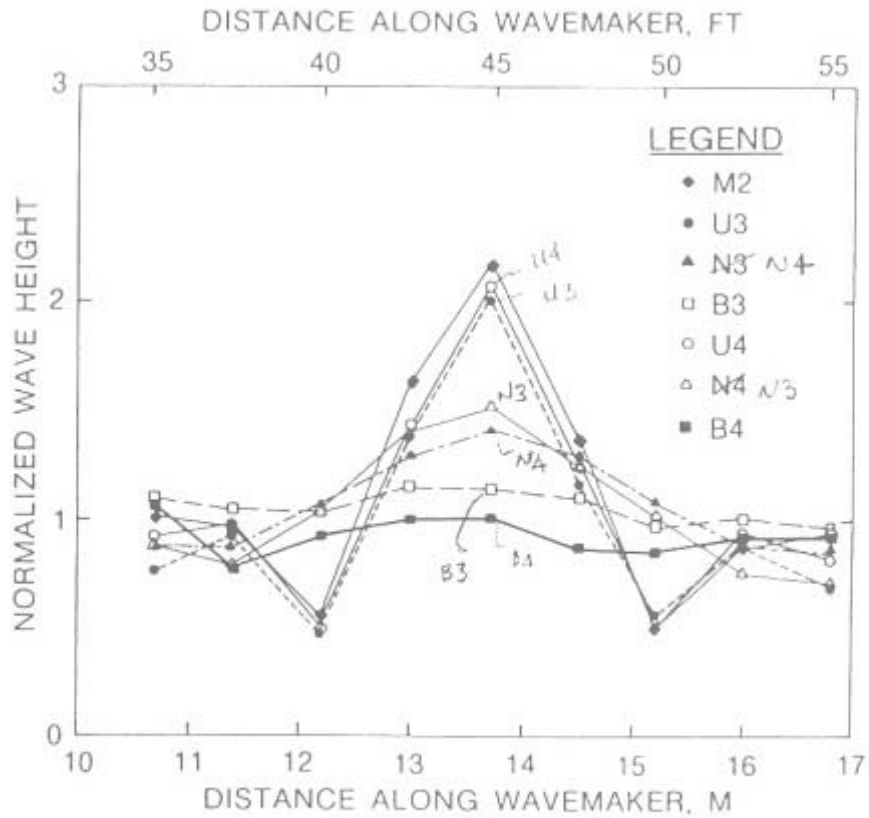


FIG. 6. Normalized Wave Heights Along Transect 4 for Non-Breaking Series Test Cases 8-14

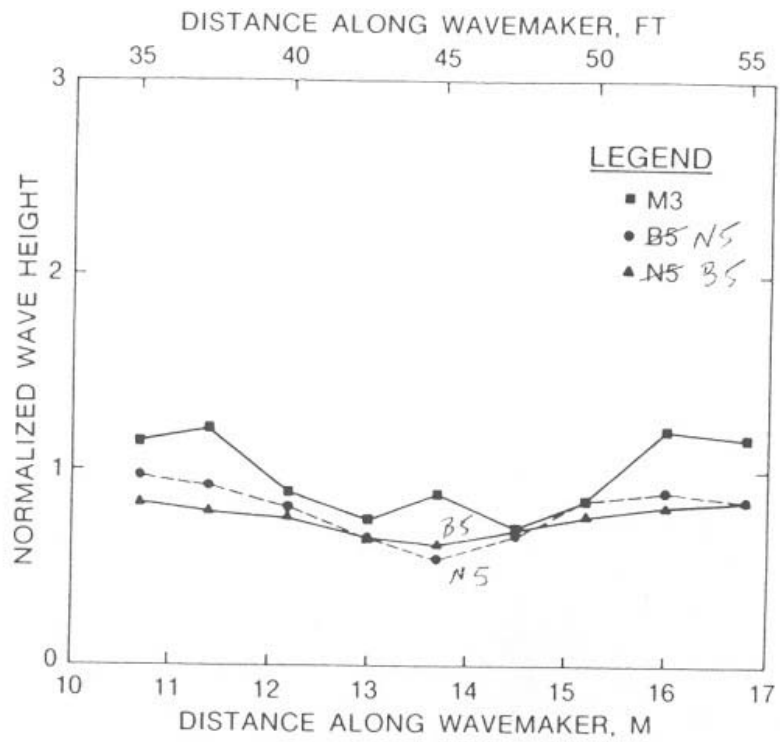


FIG. 7. Normalized Wave Heights Along Transect 4 for Breaking Series Test Cases 15-17